



## Observation of neutrons with a Gadolinium doped water Cherenkov detector

S. Dazeley<sup>a,\*</sup>, A. Bernstein<sup>a</sup>, N.S. Bowden<sup>a</sup>, R. Svoboda<sup>a,b</sup>

<sup>a</sup> Lawrence Livermore National Laboratory, 7000 East Ave, L-211, Livermore, CA 94550, USA

<sup>b</sup> Department of Physics, University of California, Davis, CA 95616, USA

### ARTICLE INFO

#### Article history:

Received 17 October 2008

Received in revised form

18 February 2009

Accepted 31 March 2009

Available online 3 May 2009

#### Keywords:

Water Cherenkov

Neutron detector

Gadolinium

Neutron capture

### ABSTRACT

Spontaneous and induced fission in Special Nuclear Material (SNM) such as  $^{235}\text{U}$  and  $^{239}\text{Pu}$  results in the emission of neutrons and high energy gamma-rays. The multiplicities of and time correlations between these particles are both powerful indicators of the presence of fissile material. Detectors sensitive to these signatures are consequently useful for nuclear material monitoring, search, and characterization. In this article, we demonstrate sensitivity to both high energy gamma-rays and neutrons with a water Cherenkov-based detector. Electrons in the detector medium, scattered by gamma-ray interactions, are detected by their Cherenkov light emission. Sensitivity to neutrons is enhanced by the addition of a Gadolinium compound to the water in low concentrations. Cherenkov light is similarly produced by an 8 MeV gamma-ray cascade following neutron capture on the Gadolinium. The large solid angle coverage and high intrinsic efficiency of this detection approach can provide robust and low cost neutron and gamma-ray detection with a single device.

© 2009 Elsevier B.V. All rights reserved.

### 1. Introduction

Many nuclear material monitoring and surveillance applications would benefit from more affordable, deployable, and environmentally benign gamma-ray and neutron counters. Long standing international nonproliferation treaties call for the tracking of nuclear materials in civil nuclear fuel cycles. More recently, there has been increased interest in the use of radiation-based screening and interrogation methods to discover illicit Special Nuclear Material (SNM) in cargo. In response, a variety of radiation portal monitors (RPM) have been developed to detect the neutrons and gamma-rays emitted by SNM, whether spontaneously or enhanced with interrogating beams.

Practical limitations, such as the need to monitor large cargo containers quickly in order to not impede legitimate commerce, require the use of large, highly efficient detection systems. Because the signature of SNM, crudely speaking, consists of several neutrons and gamma-rays emitted isotropically and in close time proximity, large solid angle coverage is imperative. This recognition has led to the use of large organic plastic or liquid scintillator detectors [1–4]. These devices have a relatively poor spectral response. As a result, these methods often rely on detecting an increase in the rate of incoming particles compared to background, rather than the analysis of the particle energy spectrum. Even without spectroscopy, rate-based approaches, such as the ‘nuclear car wash’ interrogation scheme [4], have been shown to be effective.

Well shielded SNM is difficult to detect, or may escape detection entirely, especially if the detector is sensitive to only gammas or only neutrons. A system sensitive to both gammas and neutrons is more difficult to effectively shield against, since effective gamma-ray shielding requires high Z material, while that for neutrons requires low Z material. If the dominant gamma-ray interaction in the detection medium is Compton scattering, a useful device must also be sufficiently thick to contain a significant fraction of the fission gamma-ray energy.

Although organic scintillators are attractive in many respects, they have several drawbacks. Plastic organic scintillators are expensive to build in large volumes, and difficult to dope with neutron capturing agents like Gd or  $^6\text{Li}$ . Liquid scintillator is often toxic and highly flammable. Given these limitations, water Cherenkov-based detectors offer an interesting alternative. Water is non-toxic, non-flammable and inexpensive, and retains these properties even after doping with Gadolinium or other neutron absorbing compounds. For example, the Super-K and SNO experiments [5,6] have shown that the Cherenkov process can generate enough photons to permit detection of gamma-rays with an energy greater than about 3–4 MeV – or neutron captures on chlorine – so long as the photocathode coverage is high (~40%). Neutron capture on chlorine (like Gadolinium) produces an 8 MeV gamma-ray cascade. SNO observed that the light output was approximately equivalent to a 6 MeV electron. As demonstrated here, the addition of highly reflective white walls makes it possible to detect gammas of a few MeV or more with a much smaller photocathode coverage – only about 10%.

Weapons grade Plutonium (WGPu) and highly enriched Uranium (HEU) are copious emitters of low energy (sub MeV) gamma-rays. However, if a source is located within a moderate

\* Corresponding author. Tel.: +1925 423 4792.

E-mail address: [dazeley2@llnl.gov](mailto:dazeley2@llnl.gov) (S. Dazeley).

amount of shielding, this gamma-ray signature is suppressed and difficult to detect. WGPu contains mostly  $^{239}\text{Pu}$ , and also a few percent of  $^{240}\text{Pu}$ , which spontaneously fissions, emitting approximately three neutrons on average per fission. The multiplicity (number) distribution of emitted neutrons and gamma-rays are roughly Poissonian, while the time correlations between successive neutrons and gamma-rays from the source are non-Poissonian. A large solid angle water Cherenkov detector sensitive to neutrons could detect such a source, either by registering an increase in the raw count rate or by observing a time correlation between sets of neutrons and gammas emitted in a single fission reaction or in fission chains. Methods based on interrogation with neutron or gamma beams can also benefit from this type of mixed gamma-ray/neutron detector. For example, HEU can be induced to undergo fission due to bombardment by low energy neutrons [7] or by high energy photonuclear induced fission [8]. After fission is successfully induced, the resulting unstable nuclei can produce so-called ‘ $\beta$ -delayed’ gamma-rays above 3 MeV over several tens of seconds. These high energy gamma-rays should be detectable in a water Cherenkov detector. Additionally, if such a detector were sensitive to neutron capture, it may be possible to observe time correlations between fission gammas and/or neutrons.

## 2. Detector description

Our water Cherenkov detector consists of two separate acrylic tanks. A small tank sits on top of a large tank. An O-ring between the two tanks seals the volume of the lower tank. This lower tank ( $1\text{ m} \times 0.5\text{ m} \times 0.5\text{ m}$ ) contains ultra pure, sterilized water doped with 0.2%  $\text{GdCl}_3$ . This tank forms the main 250 liter active target volume of the detector. It was fitted with a small expansion volume and airlock so that the target remains full (i.e. optically coupled to the top tank) and closed to outside air despite ambient air pressure variations. The upper tank contains ultra pure, sterilized and deionized water without the Gd dopant, and eight downward facing 8 in. ETL 9354 kb PMTs. The ETL PMTs have relatively high quantum efficiency at short wavelengths ( $\sim 30\%$ ), which is particularly advantageous for Cherenkov light detection. Our aim was to achieve a total PMT cathode coverage in the detector of approximately 10%. The PMTs face downwards into the lower tank and are individually shielded from magnetic field effects by 8 in. diameter cylinders of mu-metal. The PMT and target volumes were separated to prevent exposure of the  $\text{GdCl}_3$  doped water to the mu-metal surface – iron has been shown to react with  $\text{GdCl}_3$  in water, reducing the water clarity over time [9].

The remarkably high neutron capture cross-section of Gadolinium at thermal energies (49,000 barns) means that, even with only 0.2%  $\text{GdCl}_3$ , the mean neutron capture time is reduced to about  $30\mu\text{s}$  from the  $200\mu\text{s}$  typical of pure water (neutron capture on hydrogen). In addition, neutron capture on Gadolinium results in a gamma cascade with total energy 7.9 MeV for  $^{157}\text{Gd}$  and 8.5 MeV for  $^{155}\text{Gd}$ , resulting in an increased probability of detection.

Fig. 1 shows a schematic of the inner water detector, showing the two acrylic tanks and the PMTs inside. Two flanges are shown, the top one forming the lid of the upper small tank, the lower forming the barrier between the small upper tank, and the lower target tank. The bases of the eight PMTs are shown penetrating the top of the detector. The walls to the tanks were constructed from UV transmitting acrylic. Reflection was achieved by a combination of total internal reflection off the acrylic/outside air boundary and UV reflective 1073B Tyvek. The reflectivity of this Tyvek has been measured previously and found to be approximately 90% and 70% in the blue and UV, respectively [10,11]. The light transmissivity of our acrylic drops approximately

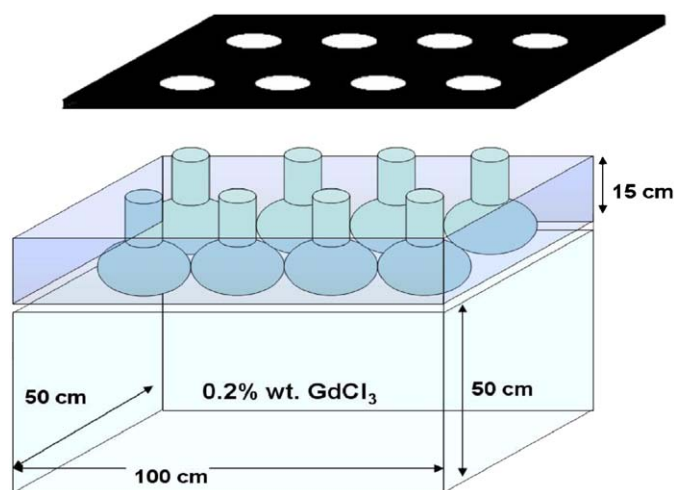


Fig. 1. Schematic design of water Cherenkov detector (see text for description).

linearly from about 90% at 400 nm to 70% at 310 nm, then drops faster to zero at approximately 280 nm. Assuming a typical Cherenkov photon spectrum in water and the transmission and reflectivity values given above, we estimate analytically that the use of UV transmitting acrylic increases the number of detected photons by an average of about 20% over regular acrylic.

The eight ETL 9354 kb PMTs operate with positive HV. The DAQ handled the signals in the following way. The anode was AC coupled and the signals sent to a pre-amp attached to the PMT base. The pre-amp signals were then routed to a 16 channel spectroscopy amplifier (CAEN N568B), which had two outputs per channel, a fast pulse and a shaped pulse. The shaped positive Gaussian pulse was sent to a peak sensing 12-bit analog to digital converter (ADC, CAEN V785), the fast pulse to a low threshold 16 channel discriminator (CAEN V814). Each PMT discriminator threshold was set to trigger at approximately 0.5 photo-electrons. Digital signals from the discriminator were processed by a CAEN V1495 FPGA module, issuing a global trigger when any four channels triggered within 100 ns. At the issue of a global trigger, all eight ADC channels were recorded to the internal 32 event buffer of the V785 together with the time since last trigger. To improve throughput, two V785 ADC were used, with triggers being sent alternately to each ADC, so that while one was performing an analog to digital conversion, the other could accept a trigger. With this arrangement a live-time of about 75% was achieved with a trigger rate of 7 kHz due to the Cf source. The dead-time of this system is mainly due to the need to pause the DAQ briefly every 64 events to empty the internal V785 buffers.

## 3. Results

We tested the ability of the device to detect both high energy gammas and neutron capture. A fission source ( $^{252}\text{Cf}$ , 55  $\mu\text{Ci}$  or  $2.4 \times 10^5$  neutrons/s) was placed on the concrete floor of the testing laboratory approximately 1 m from the detector behind a 2 in. lead wall as shown in Fig. 2. The summed PMT response from all eight PMTs is shown in Fig. 3. The raw event rate increased from 700 Hz to 7.4 kHz due to the presence of the source alone. The data rate written to disk was 5.6 kHz, due to the dead-time of 25%. The integration time was approximately 1 h. Despite the poor energy resolution characteristic to the technique, it is obvious from the figure that the presence of a  $^{252}\text{Cf}$  source changes the spectral shape, increasing the high energy ( $> 10$  photo-electrons)

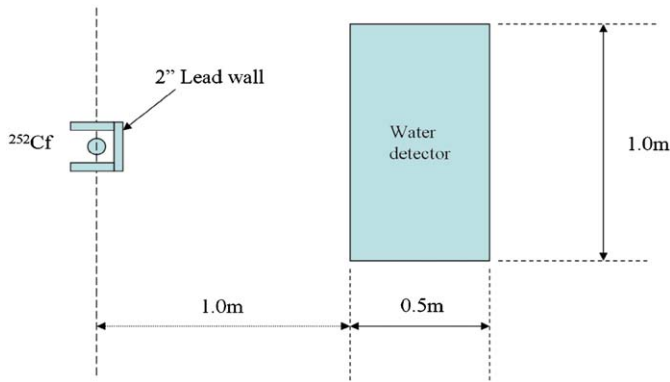


Fig. 2. Representation of the relative positions of the detector and the neutron fission source, as seen from above.

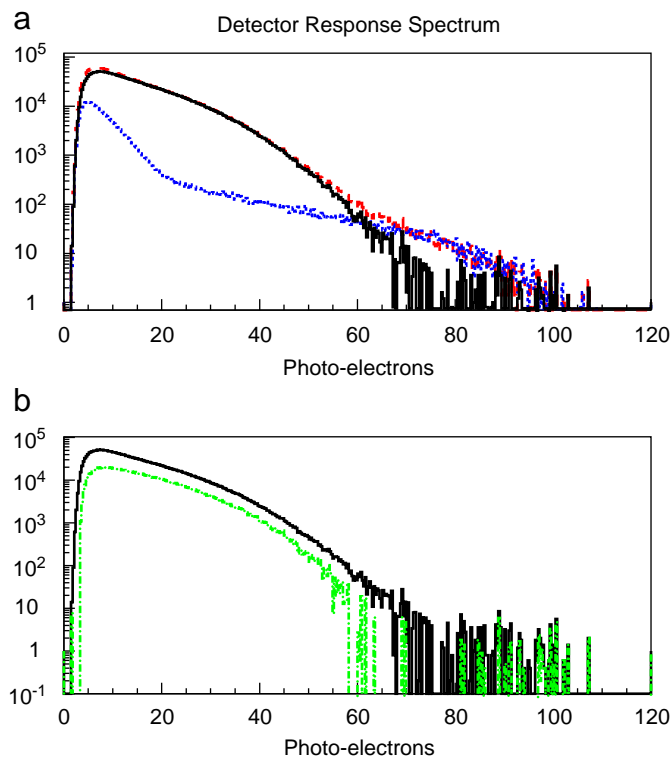


Fig. 3. The upper panel shows the summed PMT detector response spectra of our prototype with (dashed red line) and without (dotted blue line) the presence of a  $^{252}\text{Cf}$  source. The difference between the two, representing the spectrum of a pure sample of  $^{252}\text{Cf}$  source events in our prototype is shown as a solid black line in both the top and bottom panels. The green dot-dash line in the lower panel represents the statistically subtracted spectrum of pure neutron capture events in our detector.

component relative to the background. The figure also indicates that if a lower background signal is required, some improvement in signal to noise may be possible with a modest energy cut.

To test whether some of the signal that results from the  $^{252}\text{Cf}$  source is due to neutron capture, we plot the inter-event time between consecutive events in Fig. 4. Assuming Poisson statistics, the primary exponential due to uncorrelated events in the presence of the  $^{252}\text{Cf}$  source gives a corresponding event rate of 7 kHz. If we subtract this exponential, we are left with a correlated component at small inter-event times, which can be fit by another exponential, corresponding to a mean inter-event time of 28  $\mu\text{s}$ . The 28  $\mu\text{s}$  component agrees quite well with the expected mean

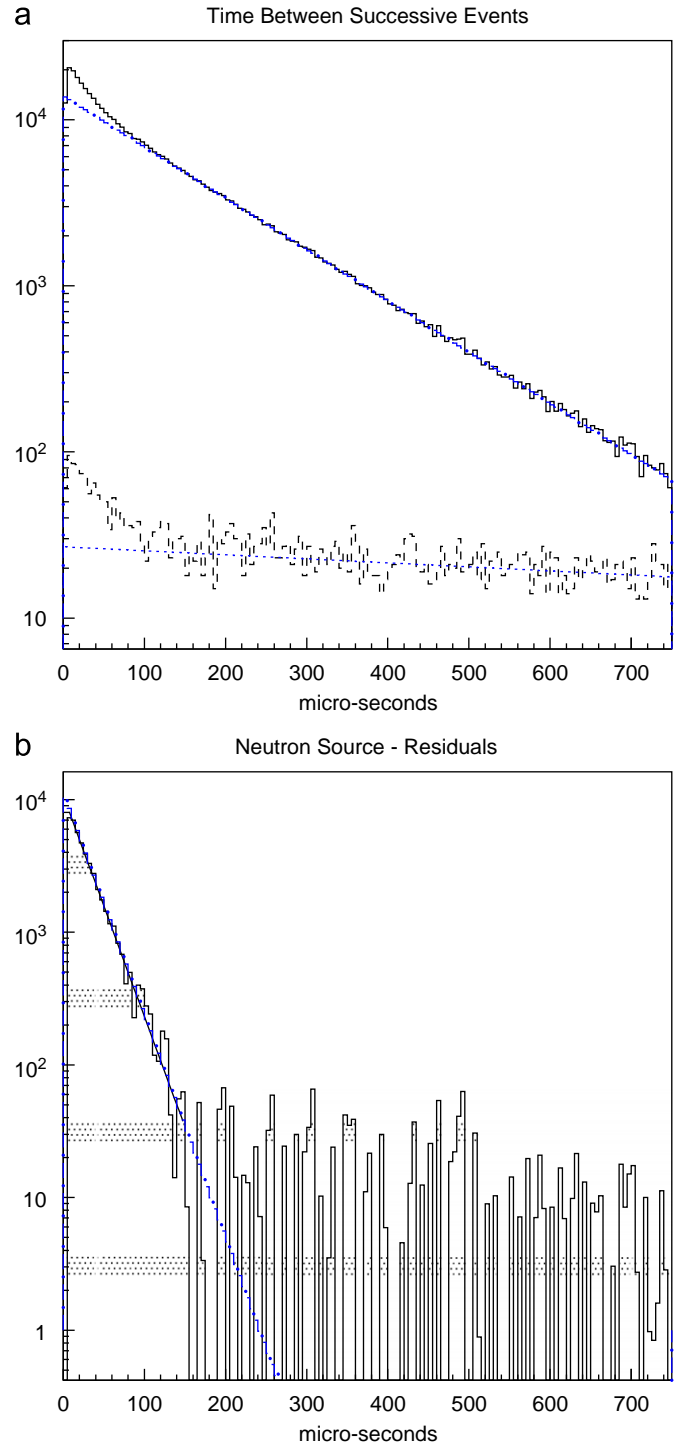


Fig. 4. Plot of the inter-event time distribution. The upper plot (a) shows the resultant distributions with and without the presence of a  $^{252}\text{Cf}$  source. The source results in an increase in both the random trigger rate and the correlated trigger rate. The lower plot (b) shows the residuals that result when the random events which were fitted by an exponential curve are subtracted, leaving only the correlated component with a mean inter-event time of 28  $\mu\text{s}$ .

neutron capture time in water or liquid scintillator (see Refs. [12–14]) for a Gadolinium concentration of 0.1% ( $\text{GdCl}_3$  concentration of 0.2%). The correlated component can be a result of either the detection of a prompt gamma-ray followed by a delayed neutron capture or a prompt neutron capture followed by a delayed neutron capture (where both particles were emitted in the same fission event in both cases). There is also a

smaller correlated neutron capture signal present when there is no  $^{252}\text{Cf}$  source present. This is due to spallation caused by the passage of muons near the detector and muon capture nearby, both of which may result in coincident gammas and neutrons, or multiple neutrons, and hence a correlation. We claim strong evidence for neutron detection in our detector on the strength of the correlated signals in Fig. 4 and the change in shape of the energy spectrum in the presence of the  $^{252}\text{Cf}$  in Fig. 3. By employing a statistical subtraction technique, it is possible to extract the spectral shape of the neutron capture events (Fig. 3b). We extracted this by taking the spectrum of a selection of  $^{252}\text{Cf}$  events correlated with a prompt signal ( $< 100\ \mu\text{s}$ ). This spectrum (the red dashed curve in Fig. 3) contained a combination of neutron capture events, fission gammas, and background gamma-rays from the local environment. We then subtracted the spectrum of a normalized selection of uncorrelated  $^{252}\text{Cf}$  events ( $> 100\ \mu\text{s}$  since previous event). The number of uncorrelated  $^{252}\text{Cf}$  events subtracted was calculated by fitting an exponential to all the uncorrelated events ( $> 100\ \mu\text{s}$ ) in the presence of the  $^{252}\text{Cf}$  source and calculating the area under the line of best fit between 0 and  $100\ \mu\text{s}$ . The remaining events reveal the spectral shape of a pure sample of correlated neutron capture events. This spectrum looks superficially similar to the neutron/gamma spectrum, indicating that our detector is not able to distinguish on an event-by-event basis between high energy fission gammas and the 8 MeV capture gamma cascade on the basis of energy alone.

#### 4. Conclusion

We have designed and built a new high energy ( $> \sim 3\ \text{MeV}$ ) fission gamma and thermal neutron detector, using a Gd doped volume of water read by PMTs. Upon exposure of the detector to a  $^{252}\text{Cf}$  source, we observed a clear signature consistent with neutrons. We also observed a correlated signal in the inter-event time distribution, again consistent with previous experiments with Gd concentration at the 0.1% level. The origin of this signal is the detection of correlated gamma-ray/neutron or neutron/neutron pairs originating from  $^{252}\text{Cf}$  fissions. We have operated the detector for several months with no evident diminution in its

sensitivity to gamma-rays or neutrons. Although Gd doped water has had a long history of being suggested for antineutrino and hence, neutron detection [15,16], ours is, we believe, the first Gd doped water Cherenkov neutron detector. This result may enable the development of cost effective, large solid angle neutron detectors, with potential nuclear nonproliferation and homeland security applications.

#### Acknowledgements

The authors would like to thank John Steele for programming the trigger logic in the FPGA. This work was performed under the auspices of the US Department of Energy by Lawrence Livermore National Laboratory under contract DE-AC52-07NA27344, release number LLNL-JRNL-405708. The authors also wish to thank the DOE NA-22 for their support of this project.

#### References

- [1] D.R. Slaughter, M.R. Accatino, A. Bernstein, et al., Nucl. Instr. and Meth. B 241 (2005) 777.
- [2] C.E. Moss, M.W. Brener, C.L. Hollas, W.L. Myers, Nucl. Instr. and Meth. B 241 (2005) 793.
- [3] J. Ely, R. Kouzes, J. Schweppe, et al., Nucl. Instr. and Meth. A 560 (2006) 373.
- [4] D.R. Slaughter, M.R. Accatino, A. Bernstein, et al., Nucl. Instr. and Meth. A 579 (2007) 349.
- [5] The Super-Kamiokande Collaboration, Phys. Rev. D 73 (2006) 112001.
- [6] The SNO Collaboration, Phys. Rev. C 72 (2005) 055502.
- [7] D. Dietrich, C. Hagmann, P. Kerr, et al., Nucl. Instr. and Meth. B 241 (2005) 826.
- [8] J.L. Jones, W.Y. Yoon, D.R. Norman, et al., Nucl. Instr. and Meth. B 241 (2005) 770.
- [9] W. Coleman, A. Bernstein, S. Dazeley, R. Svoboda, Nucl. Instr. and Meth. A 595 (2008) 339.
- [10] Surface Optics Corporation, Directional Reflectance (DR) Measurements on Two Special Sample Materials, SOC-R950-001-0195 (1995).
- [11] Surface Optics Corporation, Directional Reflectance (DR) Measurements on Five (5) UCI Supplied Sample Materials, SOC-R1059-001-0396 (1996).
- [12] M. Apollonio, et al., Eur. Phys. J. C 27 (2003) 331.
- [13] F. Boehm, et al., Phys. Rev. D 64 (2001) 112001.
- [14] A.G. Piepke, S.W. Moser, V.M. Novikov, Nucl. Instr. and Meth. A 432 (1999) 392.
- [15] J.F. Beacom, M.R. Vagins, Phys. Rev. Lett. 93 (2004) 171101.
- [16] A. Bernstein, T. West, V. Gupta, Sci. Global Security 9 (2001), 3: 235: 255.